JOURNAL OF MORPHOLOGY 270:601–614 (2009)

Stereological Estimation of the Surface Area and Oxygen Diffusing Capacity of the Respiratory Stomach of the Air-breathing Armored Catfish *Pterygoplichthys anisitsi* (Teleostei: Loricariidae)

André Luis da Cruz, Ana Carolina Elias Pedretti, and Marisa Narciso Fernandes*

Department of Physiological Sciences, Federal University of São Carlos, Caixa Postal 676, 13565-905 São Carlos, SP, Brazil

ABSTRACT The stomach of *Pterygoplichthys anisitsi* has a thin, translucent wall and a simple squamous epithelium with an underlying dense capillary network. In the cardiac and pyloric regions, most cells have short microvilli distributed throughout the cell surface and their edges are characterized by short, densely packed microvilli. The mucosal layer of the stomach has two types of pavement epithelial cells that are similar to those in the aerial respiratory organs. Type 1 pavement epithelial cells, resembling the Type I pneumocyte in mammal lungs, are flat, with a large nucleus, and extend a thin sheet of cytoplasm on the underlying capillary. Type 2 cells, resembling the Type II pneumocyte, possess numerous mitochondria, a well-developed Golgi complex, rough endoplasmic reticulum, and numerous lamellar bodies in different stages of maturation. The gastric glands, distributed throughout the mucosal layer, also have several cells with many lamellar bodies. The total volume (air + tissue), tissue, and air capacity of the stomach when inflated, increase along with body mass. The surface-to-tissue-volume ratio of stomach varies from 108 cm^{-1} in the smallest fish (0.084 kg) to 59 cm^{-1} in the largest fish (0.60 kg). The total stomach surface area shows a low correlation to body mass. Nevertheless, the body-mass-specific surface area varied from 281.40 $cm^2\ kg^{-1}$ in the smallest fish to 68.08 $cm^2\ kg^{-1}$ in the largest fish, indicating a negative correlation to body mass ($b = -0.76$). The arithmetic mean barrier thickness between air and blood was 1.52 ± 0.07 μm, whereas the harmonic mean thickness (τ_h) of the diffusion barrier ranged from 0.40 to 0.74 μm. The anatomical diffusion factor (ADF = $cm^2\ \mu m^{-1}\ kg^{-1}$) and the morphological O_2 diffusion capacity ($D_{morphol}O_2$ = $cm^3\ min^{-1}\ mmHg^{-1}\ kg^{-1}$) are higher in the smallest specimen and lower in the largest one. In conclusion, the structure and morphometric data of *P. anisitsi* stomach indicate that this organ is adapted for oxygen uptake from air. J. Morphol. 270:601–614, 2009.

KEY WORDS: air-breathing; stomach; surface area; barrier thickness; oxygen diffusion capacity

INTRODUCTION

Many fish use accessory organs to breathe air during some period or phase of their life to supply their oxygen needs, although the gills are the main gas exchange organs in teleost species. At least 49 families of teleost fish are known to have air-breathing species (Graham, 1997), most of which live in stagnant or shallow tropical and subtropical waters, employing this mode of respiration when exposed to unfavorable conditions for aquatic respiration or in response to increased oxygen requirements.

Lungfish (*Neoceratodus, Lepidosiren*) and basal actinopterygeans such as *Protoptherus* use lungs (Maina and Maloiy, 1985; Kemp, 1987; Moraes et al., 2005) and a variety of teleosts such as *Arapaima* (Sawaya, 1946), *Gymnotus* (Liem, 1989), *Hoplerythrinus* (Kramer, 1978; Mattias et al., 1996), and *Piabucina* (Graham, 1997) use the swim-bladder for air respiration. The wide variety of accessory air-breathing organs found among the higher teleosts reflects the loss of the pneumatic duct during evolution (Graham, 1997).

In the latter group, most accessory air-breathing organs are located in the region of the head and consist of the buccal and pharynx epithelia, as in *Electrophorus*, *Monopterus*, *Blennius*, and *Gobios*, pharyngeal pouches in *Channa* and *Monopterus* and modified branchial and opercular surfaces in *Clarias* and *Anabas* (Munshi, 1985). However, some air-breathing structures are located in the digestive tract (Carter and Beadle, 1931; Gee and Graham, 1978; Silva et al., 1997; Satora, 1998; Podkowa and Goniakowska-Witalinska, 1998, 2002).

Respiratory structures along the digestive tract imply regional modifications of this tract for oxy-

Contract grant sponsors: FAPESP, CNPq, and CAPES.

*Correspondence to: Marisa Narciso Fernandes, Department of Physiological Sciences, Federal University of São Carlos, Caixa Postal 676, 13565-905 São Carlos, SP, Brazil.
E-mail: dmnf@ufscar.br

Published online 23 December 2008 in
Wiley InterScience (www.interscience.wiley.com)
DOI: 10.1002/jmor.10708

gen uptake from air, including high vascularization and a thin diffusion distance between the external and internal medium. In the early 20th century, Carter and Beadle (1931) reported in some loricariid species a transparent, richly vascularized stomach that was permanently filled with air. Crawford (1974) observed the use of the esophagus as an air-breathing organ in *Dalia pectoris* and Podkowa and Goniakowska-Witalinska (2002) described the ultrastructure of the posterior intestine of *Corydoras*, emphasizing its adaptation to air breathing.

Although the functional morphological approach, together with morphometric data, are a prerequisite for understanding the function of a given organ, most morphofunctional studies of the accessory respiratory organs in air-breathing fish are so far restricted to some amphibious mudskippers (Biswas et al., 1981), Indian fishes (Hughes et al., 1974a,b; Munshi, 1985), and lungfishes (Hughes and Weibel, 1976; Maina and Maloy, 1985; Moraes et al., 2005). Recently, histological and electron microscopical studies revealed a capillary network present in the lamina propria of the mucosal layer of the stomach, subjacent to the epithelium (Silva et al., 1997; Satora, 1998; Satora and Winnicki, 2000; Oliveira et al., 2001; Podkowa and Goniakowska-Witalinska, 2003). Satora and Winnicki (2000) described the ultrastructure of *Ancistrus multispinnis* stomach, showing a dense network of capillaries, and Podkowa and Goniakowska-Witalinska (2003) determined the capillary density per 100 μm of the mucosal epithelium length and the thickness of the air-blood barrier in the stomach of *Hypostomus plecostomus*. However, the effective respiratory surface area and oxygen diffusion capacity have yet to be determined.

The main purpose of the present study was to apply stereological principles to estimate the respiratory surface area, the air-blood barrier thickness and the morphometric oxygen diffusion capacity of the stomach of the air-breathing loricariid fish *Pterygoplichthys anisitsi*. *Pterygoplichthys anisitsi* is an armored catfish occurring in South American freshwaters and is found throughout the Uruguay, Paraguay, and Paraná River basins where it inhabits water bodies characterized by low oxygen concentrations. In normoxia, this species does not breathe air during the day, but at night it increases its activity and usually swims to the surface. Under hypoxia, *P. anisitsi* breathes air even during the daytime (Cruz, 2007). Its stomach is usually full of air and sometimes contains small food particles. Preliminary observations under light microscopy showed a single epithelial cell in the mucous membrane of the stomach and a high density of capillaries close to this membrane (Oliveira et al., 2001), suggesting an adaptation to air breathing.

MATERIALS AND METHODS

Animals

Five armored catfish *Pterygoplichthys anisitsi* Eigenmann and Kennedy [body mass (M_B) = 0.084–0.600 kg; total length (L_T) = 24–39 cm] were obtained from the Aquaculture Center of the São Paulo State University (CAUNESP) at Jaboticabal, São Paulo, Brazil. In the laboratory, the fish were kept in a 1000 L aquarium with continuous water flow and aeration at 23–25°C and were fed with commercial fish food and *Lactuta sativa* leaves.

Anesthesia, Fixation, Tissue Sampling, and Processing

The fish were irreversibly anesthetized with 0.1% benzocaine® (Sinth) and the stomach was exposed through a ventral abdominal incision. The stomach was prefixed in situ with a fixative solution containing 2.5% glutaraldehyde in 0.1 M phosphate buffer pH 7.4, 300 mOsm, at 4°C. The air volume inside its lumen was measured and replaced with the same volume of fixative solution, slowly introduced into the stomach using a thin polyethylene tube through the buccal cavity and esophagus to permit replacement of air bubbles and avoid tissue stretching or distention. After tying off the esophagus and duodenum, the stomach was removed and immersed in the fixative solution for complete fixation at 4°C.

The stomach was then opened ventrally through an anteroposterior incision and the major anteroposterior and transverse lengths were measured. Tissue was taken from the open stomach according to systematic random sampling (Fig. 1a) using a square-lattice grid. The sampling sites were chosen by counting the number (N) of points lying over the open stomach and choosing every 6th/N point to sampling tissue for light and every 7th/N point for electron microscopy and marked by a pin prick. The first sampling site was chosen at random from the first six potential sites. To obtain vertical sections (VUR) and use the same section to estimate the fraction volume of stomach tissue, as well as surface density and total surface area, the external surface of the open stomach (serosa side) was considered the horizontal plane. The embedding procedures were designed so that the sections from each sample were done in a sequential +36° rotation relative to the previous one, with the first one sectioned at random between 0 and 36° (Fig. 1b,c).

The samples for light microscopy (LM) were dehydrated, embedded in Historesin® (Leica, Heidelberg, Germany) and sections of 3-μm thickness were stained with toluidine blue and fuchsin. Additional samples from cardiac, corpus, and pyloric regions of stomach were dehydrated, embedded in paraffin and sections of 5-μm thickness were stained with periodic acid Schiff and Alcian blue pH 2.5.

The samples for transmission electron microscopy (TEM) analysis were postfixed in 1% osmium tetroxide in the same buffer as before, block-stained using uranyl acetate, dehydrated in an ascending concentration of acetone, and embedded in Araldite 6005 Resin (Ladd, Burlington, VT). Semithin sections (0.5 μm) were stained with toluidine blue and the ultrathin sections (60 nm) were placed on 200-mesh copper grids, stained with uranyl acetate and lead citrate and viewed in a JEOL JEM 100 CX TEM at 80 kV.

For scanning electron microscopy (SEM) analysis, the stomachs of three other specimens were fixed as described above, ventrally opened through a median anteroposterior incision and samples from the cardiac, blind-sac (corpus), and pyloric portions were removed, dehydrated through ascending concentrations of ethanol, soaked in two successive baths of 1,1,1,3,3,3-hexamethyldisilazane (Aldrich), and air dried. The samples were glued with silver paint onto the specimen stub, coated with 99% gold (Degussa S.A) in a vacuum sputter and examined under a ZEISS-DSM 940A SEM at 25 kV.

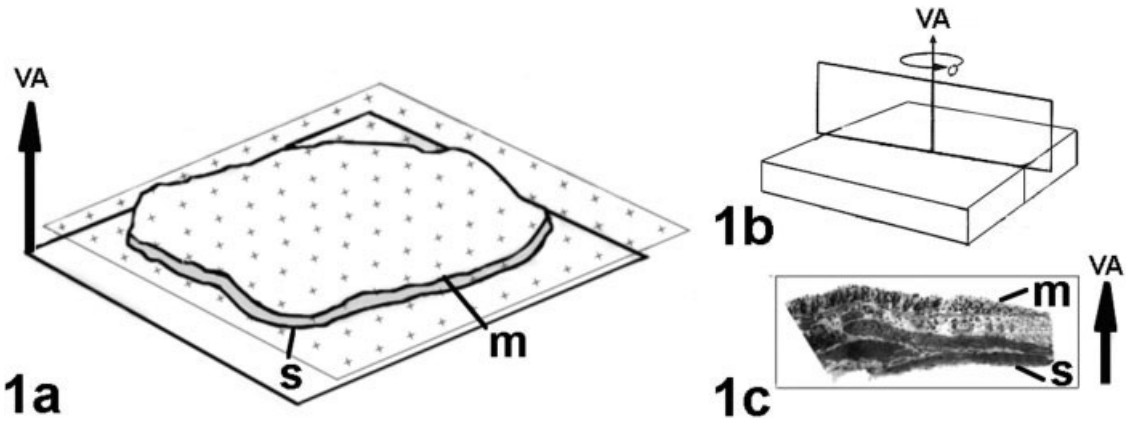

Fig. 1. Diagram of the sample scheme of stomach tissue of *Pterygoplichthys anisitsi*. (**a**) Systematic random samples from open stomach superimposed by a point square grid to obtain vertical uniform random samples. The tissue bottom is the serosa side (s) of stomach and was fixed as the horizontal plane (HP) and the vertical axis (VA) is indicated. m, mucosa. (**b**) Each tissue sample was sequentially rotated on the vertical axis (VA) and embedded. (**c**) Vertical section obtained of embedded tissue. m, mucosa; s, serosa. Arrow indicates the vertical axis (VA).

Density Volume, Surface-to-Volume Ratio, and Surface Area of Stomach

All the LM data were obtained with an Olympus BX51 light microscope, the images were captured with a JVC-TKC1380 digital video camera and analyzed using version 2.00 of the CAST System software (Olympus Denmark S/A).

The reference volume of stomach tissue (V_{St}) was calculated based on the gross surface area of opened stomach by point count of an isotropic test system superimposed on the mucosa and the stomach wall thickness obtained from vertical sections.

The differential tissue volumes of stomach were estimated using the same sections that were used for the stomach surface area ($\hat{S}_{St}$) at a final magnification of 1500×. The differential volumes or density volume [V_V (structure, reference)] of the main stomach (St) tissues (mucosa, submucosa, muscularis, serosa) were estimated by point count of an isotropic test-system, as described by Howard and Reed (1998), and was given as V_V (structure,Stomach) = (P_S 100)/P_{St}, where P_S was the number of points on the analyzed structure or tissue ($_S$) of the stomach and P_{St} was the total number of points on the stomach (St) (Fig. 2a). The density volumes of mucosa components (epithelium, capillaries, gastric gland) were estimated using the same methodology, but at higher magnification (3800×).

The stomach surface area ($\hat{S}_{St}$) was estimated from its respective surface-area-to-volume ratios ($\hat{S}v$), multiplied by the previously determined stomach volume as $\hat{S}_{St} = \hat{S}v\ V_{St}$, according to Howard and Reed (1998). The surface area-to-volume ratio ($\hat{S}v$) was estimated using a cycloid arch test system (Fig. 2a) as $\hat{S}v(\text{structure, reference}) = \frac{2\sum_{i=1}^{n} Ii}{\hat{L}}$, where Ii was the number of intersections of the test lines with the surface of mucosal surface of stomach and $\hat{L}$ was the length of test lines falling within the reference space: mucosa profile. $\hat{L}$ was estimated by multi-

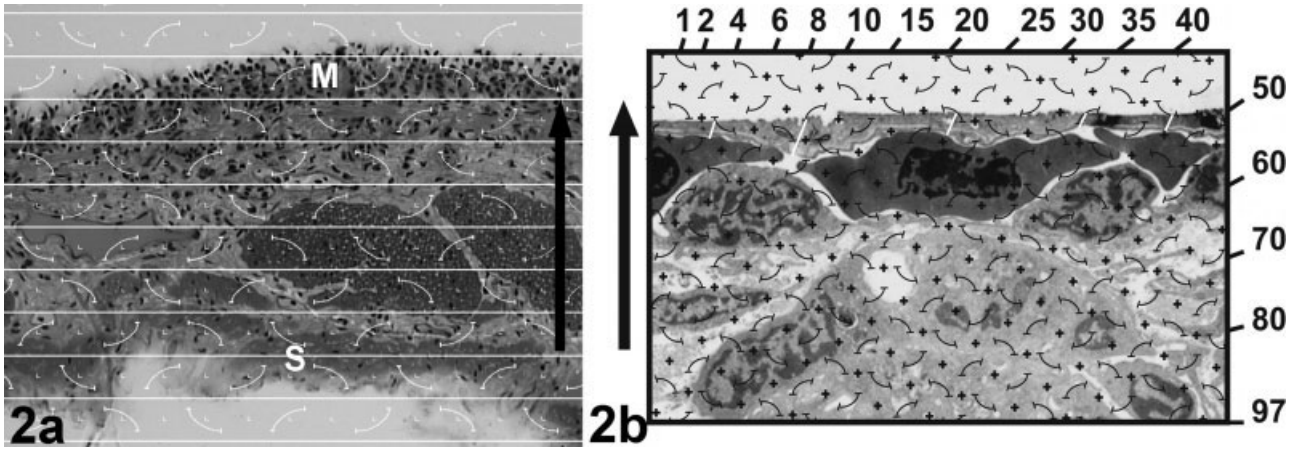

Fig. 2. (**a**) A cycloid arc test array superimposed on the microscopic image of a light micrograph in vertical section of the stomach of *Pterygoplichthys anisitsi* for the evaluation of tissue differential volumes and the surface-area-to-volume ratio. The arrow indicates the vertical axis of measurements. M, mucosa side; S, serosa side of stomach. (**b**) A cycloid arc test array superimposed on the microscopic image of TEM micrograph in vertical section of the stomach of *P. anisitsi* for the measurements of barrier thickness. For illustration, the intersection of the cycloid with the surface of mucosal layer of stomach was the starting point of measurement of barrier thickness and the line direction were the direction-number between 1 and 97 (sine-weighted line) obtained from a random number table (white line).

plying the point count for the reference space by the test line length per point.

Estimation of Air-Blood Barrier Thickness

Ultrathin sections from five stomach samples per animal were used to estimate the air-blood barrier thickness of the stomach. Subsampling of ultrathin stomach sections was based on the systematic quadrant procedure. Starting at a random position in the top left-hand corner of the TEM grid, five quadrants of ultrathin section were sampled from each grid and tissues were photographed at a magnification of 3,300×. The harmonic mean barrier thickness (τ) was measured with a logarithmic ruler and sine-weighted lines generated on the VUR sections (Gundersen et al., 1988). A new angle was selected for each sampled quadrant.

Negative film was viewed in a light box superimposed with a cycloid arch test system and a sine-weighted line to score point counts on the barrier (epithelial and endothelial cells and basal lamina) and air-blood barrier thickness (Fig. 2b). Each intersection of cycloid arc with surface of mucosal layer of stomach was the point to measure air-blood barrier distance and the line direction were the direction-number between 1 and 97 obtained from a random number table. The harmonic mean barrier thickness (Weibel and Knight, 1964) was calculated for each animal as $\tau_h = 2/3l_h$, where l_h is the harmonic mean of the lengths.

Anatomical Diffusion Factor and Morphometric Diffusion Capacity

The anatomical diffusion factor (ADF) was estimated directly from the stereological data, dividing the respiratory surface area in relation to body mass (S_R/M_B) by the harmonic mean barrier thickness (τ_h) (Perry, 1989). The morphometric diffusion capacity ($D_{morphol}$) was calculated as the product of the ADF and Krogh's diffusion coefficient (K) of the respective cell layers (epithelium, basal membrane, and endothelium) of the diffusion barrier.

Since the value of K depends on the specific gas (O_2 or CO_2), the temperature and tissue type, the K value for rat lungs was used for the epithelium and endothelium, and the K value for frog connective tissue (Bartels, 1971) was used for basal lamina. The relative volume of the epithelial and endothelial cells was estimated separately from that of basement membrane by point counting, and each element was multiplied by the appropriate K value. This weighted numerical ratio yielded a K value for oxygen (K_{O_2}) in the air-blood barrier of stomach. All values were corrected to 25°C.

Statistics

Descriptive statistics were drawn up with Microsoft's Excel spreadsheet software. The data are presented as the mean values accompanied by the respective standard errors (SEM). Since the standard deviation of a harmonic mean is not defined, the SEM was calculated from the arithmetic mean of the diffusion distance of air-blood barrier of stomach.

Regression analyses were made to seek possible significant correlations, which were calculated by the least-squares method, and the correlation coefficient (r^2) was estimated to determine the goodness of fit. The data were log transformed and the power equation: $\log Y = \log a + b \log X$ was used to calculate the scaling exponent (b), resulting in the allometric equation.

RESULTS

Stomach Morphology

Pterygoplichthys anisitsi has a short esophagus that opens into a large U-shaped stomach with a thin, translucent wall (Fig. 3a). The stomach, highly vascularized and expanded with air bubbles (Fig. 3a,b), occupies most of the volume of the coelomic cavity and was found empty in the all specimens dissected, although the intestine was full of material. Continuous to the stomach there is a long, thin, transparent intestine located ventrally to the stomach and forming several loops.

Figure 3c shows the four layers of the stomach: (1) the serosa, the outermost layer, which is characterized by a single layer of squamous epithelial cells with underlying loose connective tissue containing blood vessels; (2) the muscularis, composed of circular smooth muscles and discontinuous thick bundles of smooth muscles with longitudinal and oblique orientation among small amounts of connective tissue; (3) the submucosa, consisting of connective tissue and blood vessels of different diameters; (4) the mucosa, composed of the lamina propria containing small blood vessels, a single layer of flat epithelial cells whose apical surfaces are in contact with the stomach lumen, and the basement membrane with numerous underlying blood capillaries (Fig. 3d). Gastric glands are located in the mucous layer (Fig. 3c,d).

A SEM analysis of the mucosal surface of *Pterygoplichthys anisitsi* stomach, under low magnification, showed irregular mucosal folds in the cardiac region, longitudinal folds in the corpus region and an almost total absence of folds in the pyloric region (Fig. 4a,c, and e). Under high magnification, the epithelial pavement cells of the mucosal stomach are visibly polygonal in shape. In the cardiac and pyloric regions, most of the cells have short microvilli irregularly distributed throughout the cell surface and the boundaries of these cells are characterized by highly dense short microvilli; some cells show a smooth cell surface, in which case the cell boundary is characterized by short, continuous microridges (Fig. 4b,f). In the corpus region, the cell surfaces are smooth and the cell limits are not clearly visible (Fig. 4c). Numerous gastric gland openings are distributed among cells in all the stomach regions, but the frequency of gastric glands is lower in the corpus region (Fig. 4c,d).

The pavement epithelial cells of the stomach's mucosal layer are flat and have large nuclei, generally located between adjacent capillaries (Fig. 5a) or, rarely, elongated and located on the capillaries immediately below the basal lamina (Fig. 5b). The first cell type spreads a thin sheet of cytoplasm on the underlying capillary thus resembling the Type I pneumocyte of the mammalian lung (Fig. 5a,c). The latter cell type possesses numerous mitochondria, a well-developed Golgi complex, rough endoplasmic reticulum, and free ribosomes (Fig. 6a). Some cells contain numerous lamellar bodies in different stages of maturation therefore resembling the Type II pneumocyte (Fig. 6b,c) and numerous vesicles close to the cellular membrane

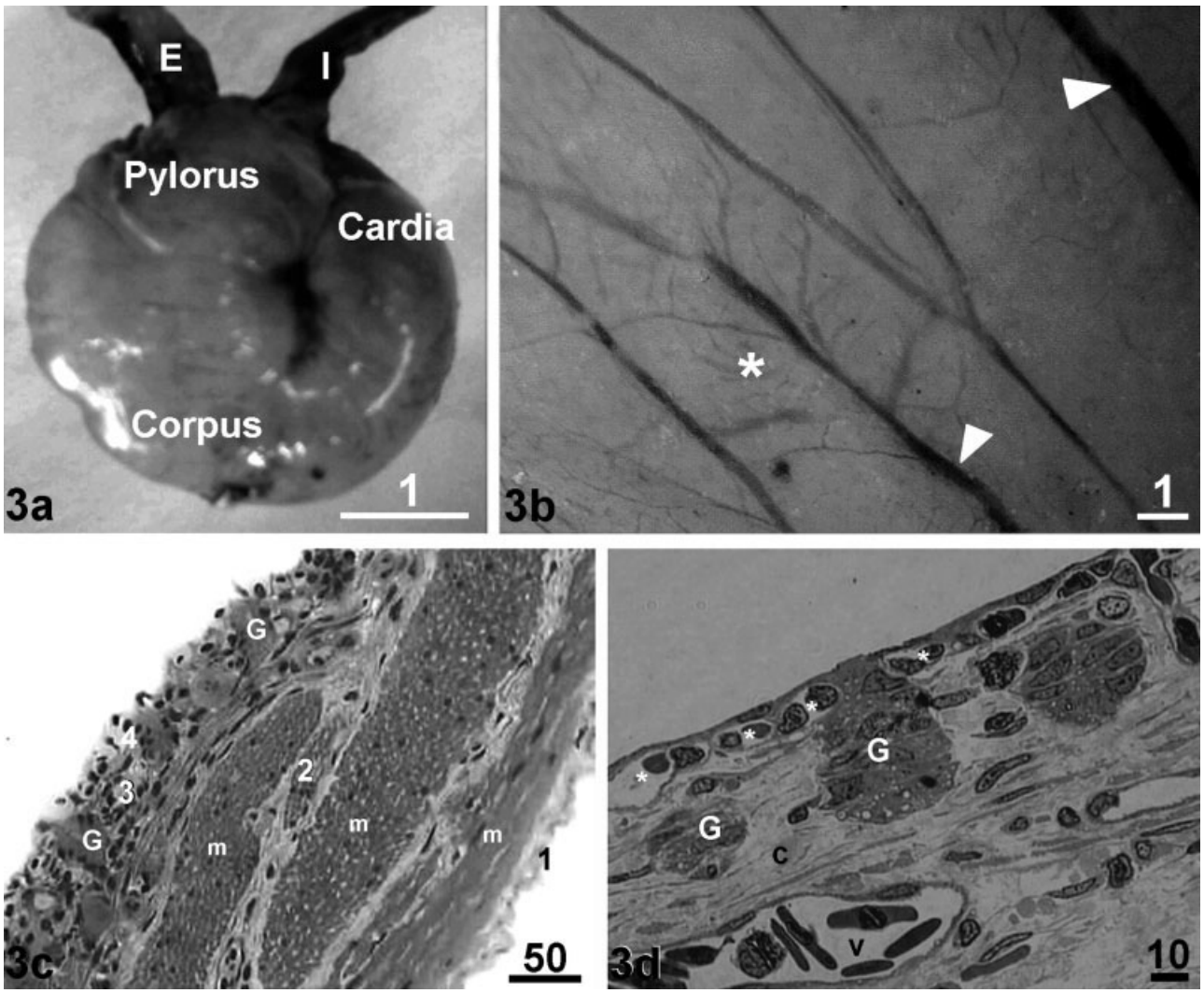

Fig. 3. (**a**) Ventral view of the stomach of *Pterygoplichthys anisitsi* full of air showing its anatomic regions: cardia, corpus, and pylorus. E, esophagus; I, intestine. Scale bar in cm. (**b**) Detail of highly vascularized stomach wall. Note large (arrowhead) and small (*) blood vessels. Scale bar in mm. (**c**) Cross section of stomach wall showing the four stomach layers, the serosa (1), muscularis (2), submucosa (3), and mucosa (4). Note gastric glands (G) in the mucosal layer. m, muscles. Scale bar in μm. (**d**) Mucosal and submucosal layers of stomach wall showing capillaries (*) underlying the epithelial cells of mucosal layer and the gastric glands (G). Small blood vessels (v) and connective tissue (c) are in the submucosal layer. Scale bar in μm.

(Fig. 6c). Some lamellar bodies have a central region composed of highly electron-dense amorphous material from which emerges a system of concentric membranes (Fig. 6b,c).

The junctional complex between two pavement epithelial cells shows a tortuous boundary because of interdigitations of each cell with its neighbor, and is characterized by a short zonula occludens and zonula adherens, generally with only one desmosome (Figs. 5b,c, and 6c). The basal lamina contacts the endothelial cells of capillaries, except in the regions where the gastric glands are present. Endothelial cells have an elongated heterochromatic nucleus protruding into the capillary lumen (Fig. 7a). Adjacent endothelial cells may overlap, showing short infolding and usually one desmosome was identified in the cell junctions. Pores of different diameters are visible in the endothelium lining the apical and lateral parts of capillaries (Fig. 5c). The air-blood barrier that separates the gastric lumen from capillaries consists of three layers, the cytoplasmic extension from epithelial cells, the basal lamina, and the sheet of endothelial cells (Figs. 5c and 6a,b).

Bundles of collagen fibers extending in different directions fill up the space between cells, blood vessels, and capillaries and the gastric glands that constitute the mucosa and submucosa (Fig. 7a); collagen fibers are found among tissues that constitute the other layers of stomach wall.

The gastric glands are regularly distributed throughout the mucosa, being more frequent in

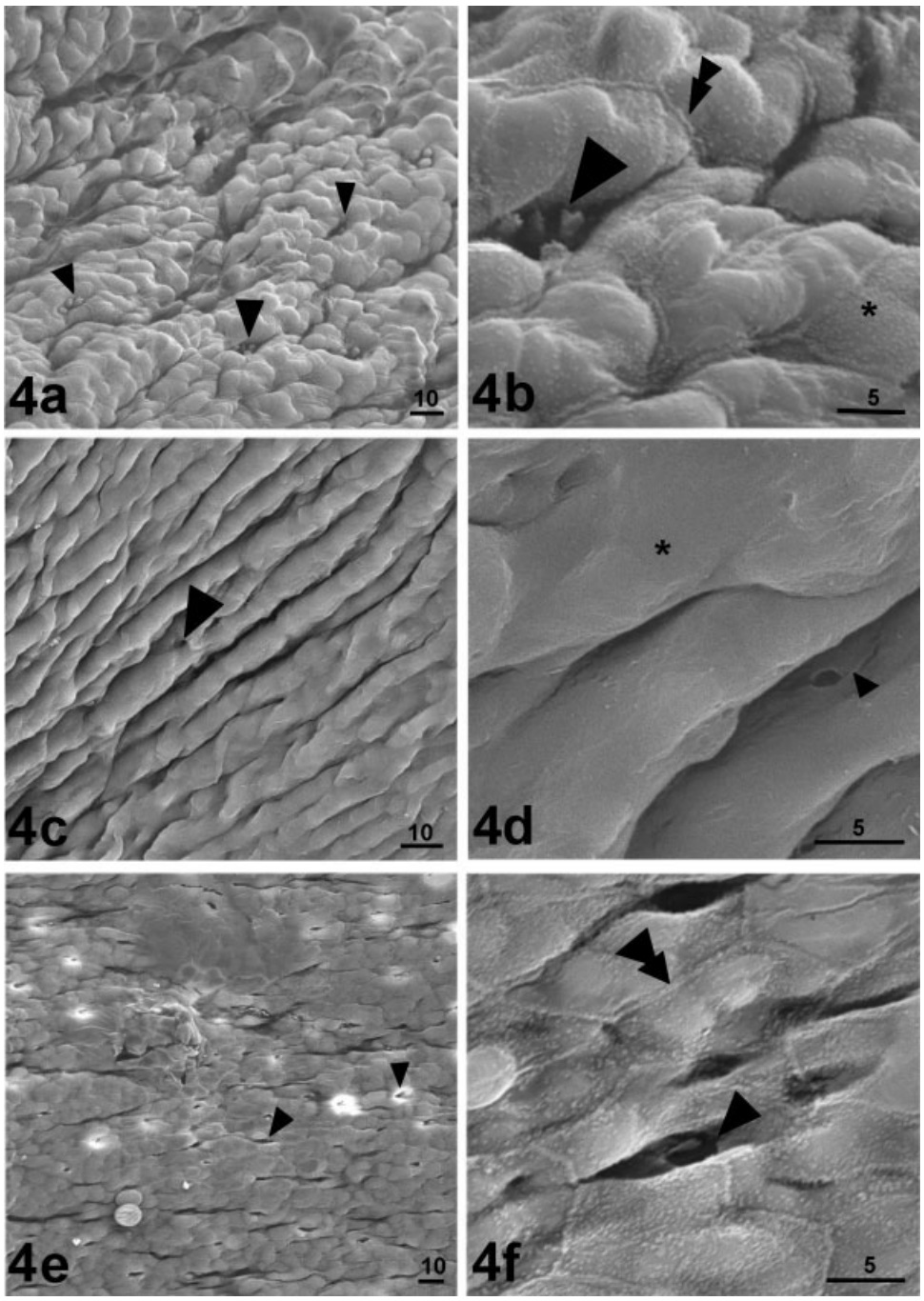

Fig. 4. Stomach regions of *Pterygoplichthys anisitsi*. SEM. Low magnification of cardiac (**a**), corpus (**c**), and pyloric (**e**) regions. The arrowheads indicate the opening of gastric glands. Scale bar in μm. High magnification of the epithelium of the mucous layer showing the pavement cell surface architecture from the cardiac (**b**), corpus (**d**), and pyloric (**f**) regions of stomach. Note the cell surface with short microvilli (*) in the (b) and (f) and a smooth surface in (d) (*). The arrowhead indicates the gastric gland opening in each stomach region and the double arrowhead the epithelial cell limits. Scale bar in μm.

the cardiac and pyloric regions, and may have a round or pyramidal shape. No morphological differences were found among the gastric glands from the three stomach regions. Although they are continuous with the epithelium, these glands nestle in the lamina propria and are surrounded by collagen fibers (Fig. 7a). The glands have 8–12 cells and each cell has a heterochromatic basal nucleus, a small number of cytoplasm organelles, and the apical region of these cells has numerous small vesicles; several cells have numerous lamellar bodies (Fig. 7a,b). The junctional complex between

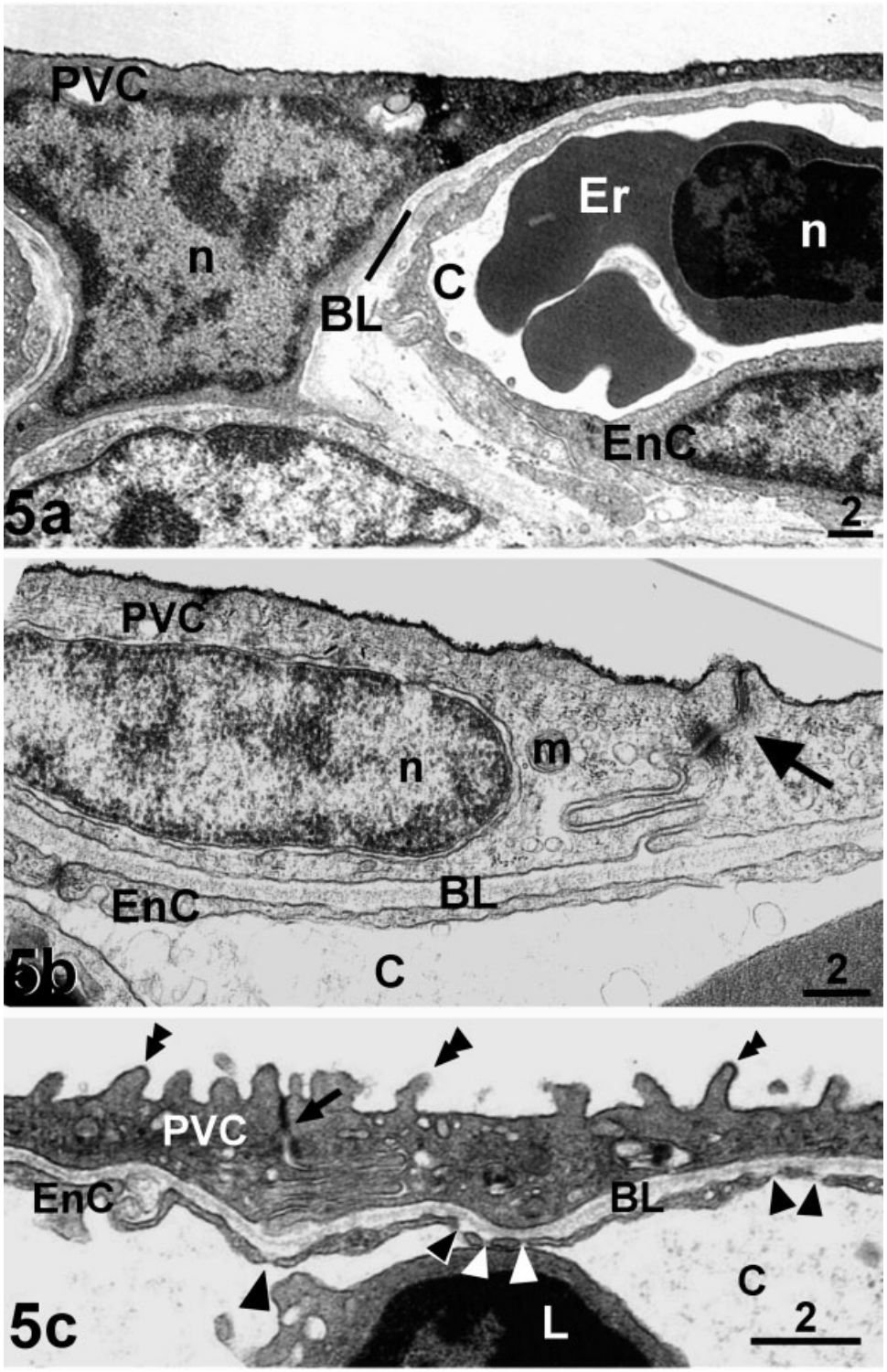

Fig. 5. Stomach mucosa of *Pterygoplichthys anisitsi*. TEM. (**a**) Pavement epithelial cell showing the cell nucleus between two adjacent blood capillaries. BL, basal lamina; C, capillary; EnC, endothelial cell; Er, erythrocyte; n, nucleus; PVC, pavement epithelial cell. (**b**) Pavement epithelial cell showing the cell nucleus on the blood capillary. Note the junctional complex (arrow) between pavement cells. BL, basal lamina; C, capillary; EnC, endothelial cell; m, mitochondria; n, nucleus; PVC, pavement epithelial cell. (**c**) Pavement epithelial cell showing the junctional complex (arrow) between cells and microvilli (double arrowheads) in the apical cell surface and the endothelial cell containing numerous pores (arrowheads). BL, basal lamina; C, capillary; EnC, endothelial cell; L, leukocyte; PVC, pavement epithelial cell. Scale bar in μm.

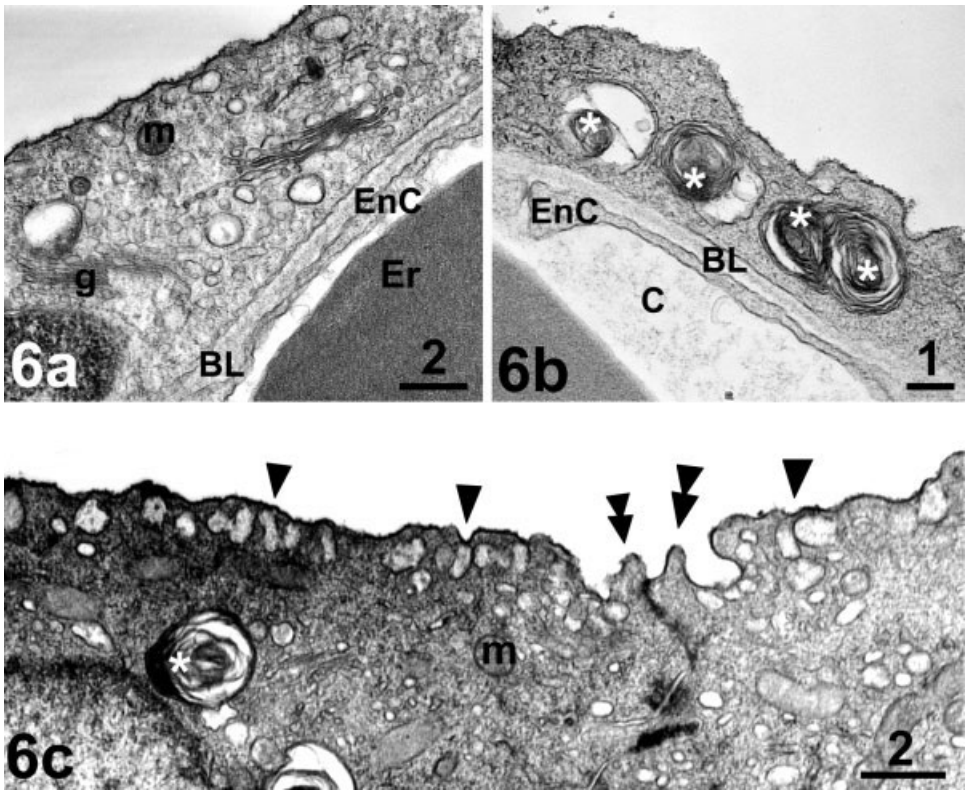

Fig. 6. Stomach mucosa of *Pterygoplichthys anisitsi* showing pavement epithelial cell resembling the Type II pneumocyte. TEM. (**a**) Cytoplasm organelles in the pavement epithelial cell. BL, basal lamina; EnC, endothelial cell; Er, erythrocyte; g, Golgi complex, m, mitochondria. (**b**) Lamellar bodies (*) with concentric membrane configuration. BL, basal lamina; C, capillary; EnC, endothelial cell. (**c**) Numerous vesicles (arrowhead) close to the apical surface of cell membrane. Note the presence of lamellar body (*) and short microvilli (double arrowheads) on the cell limit. m, mitochondria. Scale bar in μm.

these cells is characterized by intense interdigitation and several desmosomes. The negative staining with PAS and Alcian blue indicated that these glands do not produce acid and neutral mucopolysaccharides. Rare endocrine cells are found together with the gastric glands and are characterized by electron-lucent cytoplasm with electron-dense vesicles (Fig. 7b,c).

Stomach Morphometry

The mean anteroposterior and transversal length of stomach of *Pterygoplichthys anisitsi* in 0.084–0.60 kg-fish were 6.5 ± 0.87 and 5.03 ± 0.61 cm, respectively. Of the 20.245 ± 4.747 cm^3 which corresponds to the stomach's total mean volume (air + tissue), only 0.425 ± 0.080 cm^3 represents the stomach tissue, and the total stomach volume to body mass ratio is 85.21 ± 14.09 cm^3 kg^{-1}. The volume of stomach tissue, air volume capacity and the total volume (air + tissue) of inflated stomach (Table 1) increased with body mass, whereas the specific stomach volume (V_{St} M_B^{-1}) decreased according to the power equation $V = aM_B^b$, where V is the tissue (ts,St), air (air,St), or total (St) volumes of stomach, M_B is the body mass, a is the value for 1 g fish and b is the scaling or mass coefficient (Table 2). In the log form: $\log V = \log a + b \log M_B$, the stomach volume describes a straight line where a is the intercept and b is the slope (Table 2). The percentage of volume densities of stomach tissue layers of *P. anisitsi* is depicted in Figure 8a. The muscle layers represent the major volume density of stomach tissue, followed by the submucosa, mucosa and serosa layers. Considering only the mucosa together with the lamina propria, the capillaries and the gastric glands represent 34 and 46%, respectively, of the volume of this layer (Fig. 8b).

The surface-to-tissue-volume ratio of *Pterygoplichthys anisitsi* stomach varies from 108 cm^{-1} in the smallest fish (0.084 kg) to 59 cm^{-1} in the largest fish (0.60 kg). The mean total stomach surface ($\hat{S}_{St}$) (Table 3) increased with body mass, but showed a low correlation with body mass ($\hat{S}_{St}$ = 42.01 $M_B^{0.23}$, r^2 = 0.33). Nevertheless, the specific surface area ($\hat{S}_{St}$ M_B^{-1}) varied from 281.40 cm^2 kg^{-1} in the smallest fish to 68.08 cm^2 kg^{-1} in the largest one, showing a negative correlation with body mass ($\hat{S}_{St}$ M_B^{-1} = 42.02 $M_B^{-0.76}$, r^2 = 0.84, $P < 0.05$).

The mean value of barrier thickness between air and blood (arithmetic mean) was 1.52 ± 0.07 μm,

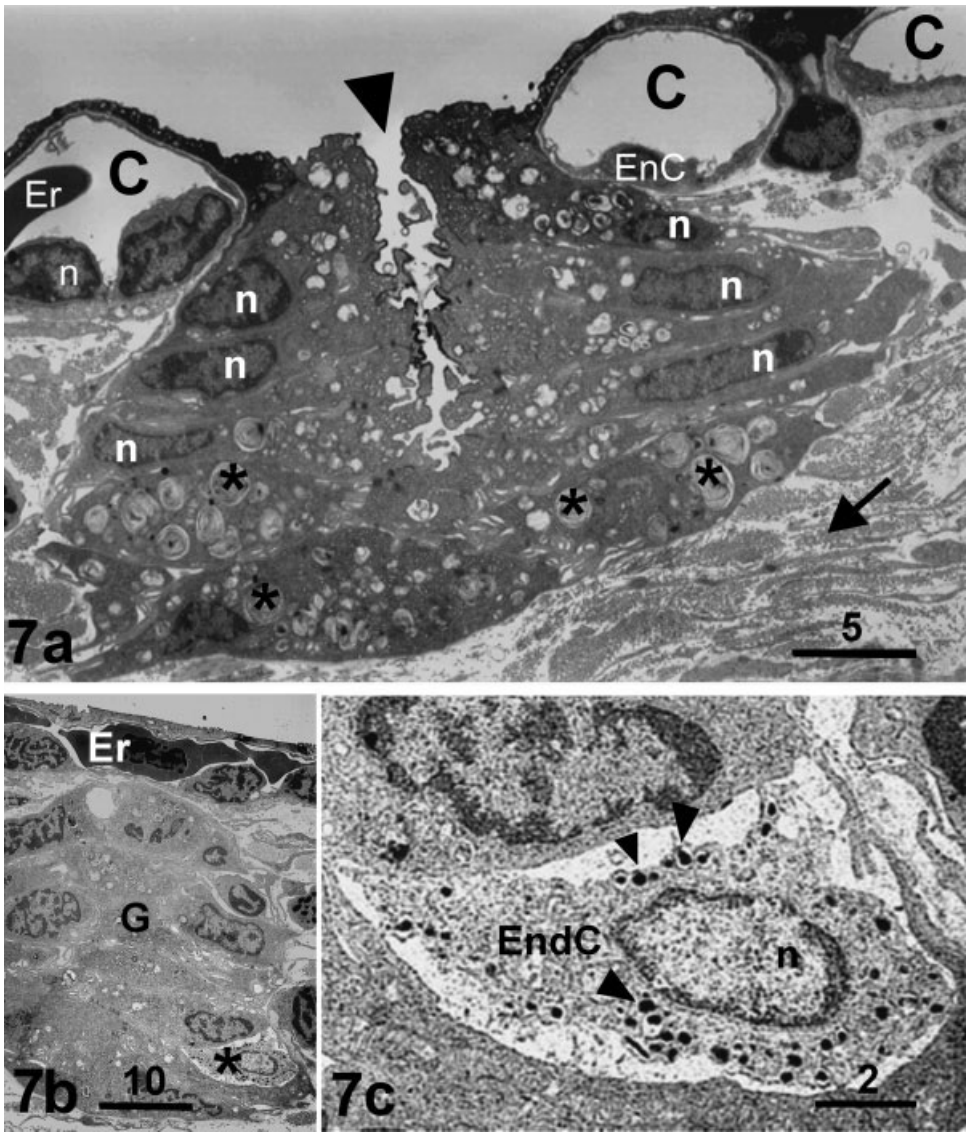

Fig. 7. (**a**) Gastric gland opened (arrowhead) in the mucosal layer of stomach of *Pterygoplichthys anisitsi*. Note the gastric gland organization, nucleus position, and numerous lamellar bodies (*) in these cells. Arrow indicates collagen fibers. C, capillary; EnC, endothelial cell; Er, erythrocyte; n, nucleus. (**b**) Part of gastric gland (G) in the submucosal layer of stomach showing endocrine cell (*). (**c**) High magnification of endocrine cell showing electron-dense bodies (arrowheads) distributed in the cytoplasm and close to the cell membrane. EndC, endocrine cell. Scale bar in μm.

whereas the harmonic mean thickness (τ_h) of the diffusion barrier ranged from 0.40 to 0.74 μm. The specific anatomical diffusion factor (ADF = $\hat{S}_{St}\ \tau_h^{-1}$ M_B^{-1}) and the morphological O_2 diffusion capacity were higher in the smallest specimen and lower in the largest one (Table 3).

TABLE 1. Range and mean (±SEM) of the body mass and length, the air ($V_{air,St}$), tissue ($V_{ts,St}$), and total ($V_{Total,St}$) volume of stomach and total specific stomach volume ($V_{Total,}St\ M_B^{-1}$) of Pterygoplichthys anisitsi (n = 5)

	Range	Mean	SEM
Body mass (kg)	0.084–0.600	0.285	0.096
Body length (cm)	23–42	31.8	3.39
$V_{air,St}$ (cm^3)	11.3–35.0	19.320	4.692
$V_{ts,St}$ (cm^3)	0.225–0.611	0.425	0.080
V_{St} (cm^3)	11.519–35.611	20.245	4.747
$V_{St}\ M_B^{-1}$ ($cm^3\ kg^{-1}$)	137.13–59.35	85.21	14.09

DISCUSSION

This is the first morphometric study of the stomach of an air-breathing fish, with special emphasis on the respiratory function. Our results show the morphological adaptation of *Pterygoplichthys anisitsi* stomach to gas exchange. We estimated the respiratory surface area of this organ and the morphometric diffusion capacity for oxygen.

TABLE 2. Relationships between tissue ($V_{ts,St}$), air ($V_{air,St}$), and total (V_{St}) volumes of stomach and body mass (M_B) of Pterygoplichthys anisitsi (M_B = 0.084–0.600 kg, n = 5)

$V = aM_B^b$	$\log V = \log a + b \log M_B$	r^2	P
$V_{ts,St} = 0.825M_B^{0.568}$	$\text{Log } V_{ts,St} = -0.083 + 0.568\log M_B$	0.93	0.05
$V_{air,St} = 45.219M_B^{0.625}$	$\text{Log } V_{air,St} = 1.655 + 0.625\log M_B$	0.90	0.05
$V_{St} = 46.018M_B^{0.621}$	$\text{Log } V_{St} = 1.663 + 0.621\log M_B$	0.91	0.05
$V_{St}\, M_B^{-1} = 46.018M_B^{-0.379}$	$\text{Log } V_{St}\, M_B^{-1} = 1.660 - 0.379\log M_B$	0.80	0.05

Stomach Morphology

Although fish present a high diversity of digestive tracts relating to diet and feeding habits, the stomach of teleosts generally has a thick wall consisting of a serosal layer, a discontinuous muscular layer, a submucosa and mucosal layers; the mucosal layer is characterized by a simple columnar epithelium (Morrison and Wright, 1999) and gastric glands that usually have two cell types, the electron-lucent cytoplasm cells that produce hydrochloric acid and the electron-dense cytoplasm cells that produce pepsinogen (Elbal and Agulleiro, 1986).

In loricariid fish, most of which are herbivorous or detritivorous species, the stomach is little developed and the intestine is long (Delariva and Agostinho, 2001). Several species of this family use the stomach or intestine as an auxiliary organ to breathe atmospheric air (Mattias et al., 1996; Graham, 1997; Cruz, 2007) and they exhibit great diversity in the anatomical morphology of the respiratory function (McMahon and Burggren, 1987; Silva et al., 1997; Satora, 1998). However, a thin pavement epithelial cell with an underlying dense capillary network in the mucosal layer characterizes tissue adaptation to gas exchange. In *Pterygoplichthys anisitsi* the stomach is modified for air breathing; it is large, translucent, highly vascularized, and is usually empty of food particles but full of air, very similar to the stomach described for the air-breathing loricariid *Ancistrus multispinnis* (Satora and Winnicki, 2000), *Hypostomus plecostomus* (Podkowa and Goniakowska-Witalinska, 2003) and the aerial sacs of *Loricarichthys platymetopon* stomach (Silva et al., 1997).

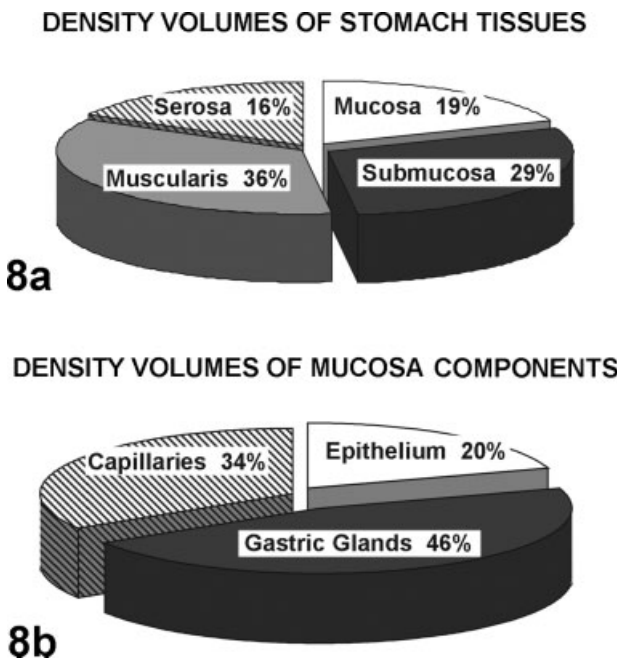

Fig. 8. Stomach of *Pterygoplichthys anisitsi*. (**a**) Percentage volumes of the stomach tissues components. (**b**) Percentage volumes of epithelium, capillaries, and gastric glands in the mucosal layer of the stomach.

The SEM images revealed three stomach epithelial regions in the apparently poorly differentiated mucosal layer of *Pterygoplichthys anisitsi* stomach, which suggest a possible characteristic reminiscent of typical stomachs. The absence of epithelial Alcian blue-positive and PAS-positive cells indicates that acid and neutral mucopolysaccharides are not synthesized in the stomach. In a typical stomach, mucus protects the epithelial cells from mechanical injuries and enzyme activity. Although numerous gastric glands having several vesicles are distributed throughout the mucosal layer of stomach, they do not present zymogen granules, suggesting that intensive food digestion occurs in the long intestine instead of stomach, as already pointed out by Podkowa and Goniakowska-Witalinska (2003) for *Hypostomus plecostomus*, a loricariid fish with similar feeding habits. The role of the rare endocrine-like cells characterized by small vesicles with electron-dense material observed in *P. anisitsi* only together with the gastric glands, as in *Loricariichthys platymetopon* (Silva et al., 1997), is unknown since food digestion does not seem to occur in the stomach. Podkowa and Goniakowska-Witalinska (2003) did not exclude a possible role of these cells in the local regulation of the respiratory function.

The ultrastructure of pavement epithelial cells of the mucosal layer of *Pterygoplichthys anisitsi* stomach is similar to those described for the respiratory aerial sacs of *Loricariichthys platymetopon* (Silva et al., 1997), the stomach of *Ancistrus multispinnis* (Satora and Winnicki, 2000) and *Hypostomus plecostomus* (Podkowa and Goniakowska-Witalinska, 2003), the swim bladder of the catfish *Pangasius hypophthalmus* (Podkowa and Goniakowska-Wita-

TABLE 3. Range and mean values (±SEM) of the surface to volume ratio ($\hat{S}v_{St}$), the surface area ($\hat{S}_{St}$), specific surface area of stomach ($\hat{S}_{St}\,M_B^{-1}$), arithmetic mean of the air-blood diffusion barrier (τ_{arith}), harmonic mean (τ_h), anatomic diffusion factor (ADF) and morphometric diffusion capacity for O_2 ($D_{morphol}O_2$) of stomach of Pterygoplichthys anisitsi (n = 5)

	Range	Mean	SEM
$\hat{S}v_{,St}$ (cm^{-1})	58.62–107.79	77.14	8.33
$\hat{S}_{St}$ (cm^2)	19.80–40.85	30.76	4.15
$\hat{S}_{St}\,M_B^{-1}$ ($cm^2\ kg^{-1}$)	68.08–281.40	157.21	45.34
τ_{arith} (μm)	1.36–1.82	1.52	0.07
τ_h (μm)	0.40–0.74	—	—
ADF ($cm^2\ \mu m^{-1}\ kg^{-1}$)	103.15–703.57	333.95	102.06
$D_{morphol}O_2$ ($cm^3\ min^{-1}\ mmHg^{-1}\ kg^{-1}$)	0.122–0.0487	0.0874	0.0291

linska, 1998), and the lungfish lungs (Maina and Maloiy, 1985; Moraes et al., 2005). Most of the epithelial cells of *P. anisitsi* stomach resemble the Type I pneumocyte of mammal lungs and some of them present characteristics of the Type II pneumocyte, exhibiting lamellar bodies in their cytoplasm. Lamellar bodies have been described in epithelial cells of the air-breathing organs of fish such as the stomach (Silva et al., 1997; Satora, 1998), intestine (Podkowa and Goniakowska-Witalinska, 2002), and swim bladder (Podkowa and Goniakowska-Witalinska, 1998) without distinction among epithelial cell types. This finding opens a question about the derivative characteristic of amniotes as these cell types have been described in the lung epithelium of higher vertebrates. The lung is a derivative of the gut (foregut endoderm) and the lamellar bodies have been described as the site of surfactant accumulation and are highly morphologically and biochemically conserved throughout the radiation of air-breathing organs among vertebrates (Daniels et al., 2004). Further biochemical and physiology studies are needed to establish similarity, beyond considering only morphological characteristics. In *P. anisitsi* lamellar bodies are also found distributed in the cytoplasm of gastric gland cells.

Lamellar bodies have been described as the site of surfactant accumulation (Daniels et al., 2004) that is discharged by exocytosis into the respiratory organ lumen. The thin film of this substance over the luminal surface of the respiratory organ reduces the forces of attraction between the water molecules at the surface film, thereby decreasing the surface tension and favoring oxygen absorption (Orgeig and Daniels, 2001). Furthermore, this substance may be involved in the antimicrobial defense mechanisms of respiratory organs (Daniels et al., 1995; Rubio et al., 1996) and prevent epithelial desiccation and oxidative damage of epithelial cells (Daniels and Orgeig, 2001).

The structure of the air-blood diffusion barrier of respiratory epithelium of the stomach of *Pterygoplichthys anisitsi* consisted of the same structures as the respiratory epithelium of the lungs of other vertebrates. The triple membrane model (epithelium, basal membrane, and endothelium) of the diffusion barrier characterizes the air-blood barrier of respiratory organs of vertebrates (Maina and West, 2005) and the accessory organs for air breathing in fish. Most endothelial cells of the capillaries underlying the basal membrane may be classified as continuous and are characteristic of the respiratory organs; fenestrated capillaries that are characteristic capillaries of the digestive tract are also observed in the stomach of *P. anisitsi* as in *Hypostomus* (Podkowa and Goniakowska-Witalinska, 2003) and in the respiratory regions of the intestine of *Corydoras* (Podkowa and Goniakowska-Witalinska, 2002). However, independent of the type of capillary underlying the mucosal epithelium of the stomach, the distance between air and blood is similar to the distance in the lungs of aerial vertebrates, indicating that the stomach is the auxiliary organ for breathing air in *P. anisitsi*.

Stomach Morphometry

The air volume of stomach ($V_{air,St}$) of *Pterygoplichthys anisitsi* between 11.3 and 35.0 cm^3 for fish weighing from 84 to 600 g and with 23 to 42 cm length is congruent with that reported by Gee (1976) for other loricariid fish, and also shows a positive correlation between body mass and air ($V_{air,St}$), tissue ($V_{ts,St}$) and total (V_{St}) stomach volume. A negative correlation between body mass and specific total volume ($V_{St}\,M_B^{-1}$), as expected, is consistent with most biological parameters in animals.

The low percentage volume of the mucosal and serosal layers of stomach and the high volume density of the capillary underlying the epithelium in the mucosal layer are similar to those found in the tissue volumes of the respiratory organs of other animals. In lungs, the volume of parenchymal tissue specialized in gas exchange (respiratory epithelium) occupies a low volume density (Burri et al., 2003) and the capillary density is higher than the density of epithelium (Burri et al., 2003; Moraes et al., 2005).

The potential efficiency of the *Pterygoplichthys anisitsi* stomach as a respiratory organ is high considering the simplicity of its structure. In the South American lungfish *Lepidosiren paradoxa*

TABLE 4. Specific surface area ($\hat{S}_{St}\,M_B^{-1}$), harmonic mean of the water-blood diffusion barrier (τ_h) and morphometric diffusion capacity for O_2 ($D_{morphol}O_2$) of the air-breathing organs in fish

Animal	Air-breathing organ	$\hat{S}_{St}\,M_B^{-1}$ ($cm^2\ kg^{-1}$)	τ_h (μm)	$D_{morphol}O_2$ ($cm^3\ min^{-1}\ mmHg^{-1}\ kg^{-1}$)
Clarias batrachus (Munshi, 1985)	Suprabranchial Chambers (SBC)	155	—	0.0420
	Gill fans	34	—	0.0005
	Arborescent organ	287	0.55	0.0773
Heteropneustes fossilis (Hughes et al, 1974a)	Air sac	310	1.605	0.0288
Monopterus cuchia (Hughes et al., 1974b)	Air sac	48	0.44	0.0165
Channa punctatus (Hakin et al., 1978)	SBC	392	0.780	0.0753
Channa striatus (Munshi, 1985)	SBC	231	1.359	0.0254
Channa gachua (Munshi, 1985)	SBC	195	0.56	0.0524
Pangasius hypophthalmus (Padkova and Gonialowska-Witalinska, 1998)	Swimbladder	—	0.7	—
Hypostumus plecostomus (Padkova and Gonialowska-Witalinska, 2003)	Stomach	—	0.86	—
P. anisitsi (present study)	Stomach	157	0.40–0.74	0.0874
Protopterus aethiopcus (Maina and Maloiy, 1985)	Lungs	14000	0.37	13.035
Lepidosiren paradoxa (Hughes and Weibel, 1976)	Lungs	850	0.86	0.3
Lepidosiren paradoxa (Moraes et al., 2005)	Lungs	664	1.38	0.110

(Moraes et al., 2005) and some reptiles, birds and mammals (Perry, 1989) that depend exclusively on the pulmonary structure to obtain the oxygen needs for metabolism, the potential respiratory surface corresponds to higher values. Compared with the exclusively air-breathing animals, our results are evidence that *P. anisitsi* depends on the potential respiratory surface of the stomach for aerial respiration only under adverse conditions in which aquatic respiration does not supply its needs. The 1.5 times higher $\hat{S}v$ of stomach of small fish and the decreasing specific surface area with increasing body mass suggest that small animals would be capable of obtaining greater specific oxygen uptake from atmospheric air than larger specimens.

The arithmetic (τ_{arith}) and harmonic (τ_h) mean of the thickness of the air-blood diffusion barrier of *Pterygoplichthys anisitsi* stomach lies in the range of most air-breathing organs of fish such as the arborescent organ of *Clarias batrachus* (Munshi, 1985), the air sac of *Heteropneustes fossilis* (Hughes et al., 1974a) and *Monopterus cuchia* (Munshi et al., 1989), the suprabranchial chambers of *Channa punctatus* (Hakin et al., 1978), *C. striatus* and *C. gachua* (Munshi, 1985), the swim bladder of *Pangasius hypophthalmus* (Podkowa and Goniakowska-Witalinska, 1998), and the stomach of *Hypostumus plecostomus* (Podkowa and Goniakowska-Witalinska, 2003), and is lower than the lung of the South American lungfish, *Lepidosiren paradoxa* (Hughes and Weibel, 1976; Moraes et al., 2005) (Table 4). The low values of the diffusion barrier of respiratory organs evidence the preservation of the barrier model in different groups of animals that breathe air to allow for an efficient gas exchange process, as emphasized by Maina and West (2005).

The ADF, which is the ratio of the respiratory surface area to the harmonic mean of the diffusion barrier (Perry, 1989), represents the anatomical component of the diffusion capacity of a respiratory tissue, excluding the blood. The ADF of the stomach of *Pterygoplichthys anisitsi* is smaller than that of the lungs of most vertebrates, which increase from amphibians to mammals (Perry, 1992), but similar to those of the lungfish (Hughes and Weibel, 1976; Moraes et al., 2005). The stomach of *P. anisitsi* has a low specific stomach surface area ($\hat{S}_{St}\,M_B^{-1}$) but its air-blood barrier is thinner than that of the lung of *Lepidosiren paradoxa* (Moraes et al., 2005) (Table 4).

The $D_{morphol}$ of tissue barrier of stomach of *Pterygoplichthys anisitsi* is higher than the air-breathing organs of most air-breathing fish but lower than the lung of lungfish (Table 4). $D_{morphol} = K(S/t)$, where K is the Krogh specific diffusion constant for O_2 or CO_2, S is the respiratory surface area, and t is the harmonic mean of the diffusion barrier thickness, represents the maximum diffusion capacity of a given respiratory organ under ideal conditions of ventilation/perfusion in the entire diffusion barrier. On the other hand, $D_{physiol} = VO_2/(PaO_2 - PeO_2)$, where VO_2 is the oxygen consumption rate, PaO_2 is the arterial partial oxygen tension, and PeO_2 is the venous partial oxygen tension, represents the diffusion capacity under specific physiological conditions, considering the differences in the ventilation/perfusion ratio and the heterogeneity of diffusion membrane barrier. The $D_{morphol}$ is usually much higher than the estimated $D_{physiol}$, which approximates the $D_{morphol}$ only during extreme exercise or in combination with hypoxia and/or hypercapnia (Scotto et al., 1987; Weibel, 1999). The $D_{morphol}$ of the stomach of *P. anisitsi* showed a structural and functional simi-

larity in the characteristics of respiratory tissues specialized in using atmospheric air for gas exchange (very thin diffusion barrier), and a pattern for ectothermic animals which present low activity (low respiratory surface area).

In conclusion, the structure and morphometric data of *Pterygoplichthys anisitsi* stomach demonstrate the adaptation of this organ to gas exchange from air. Moreover, considering that this species is a continuous but non-obligatory air-breathing fish (Cruz, 2007) that uses its stomach as an auxiliary organ in response to hypoxia because of extremely poor dissolved oxygen in water, and that atmospheric air contains 35 times more oxygen than air-saturated freshwater, the morphological and morphometric properties of the stomach of *P. anisitsi* enable this species to live in severely hypoxic environments, since it can obtain O_2 from air to supply its metabolic needs.

ACKNOWLEDGMENTS

The authors thank the Aquaculture Center of the São Paulo State University, Jaboticabal campus, for providing the fish. They also thank the anonymous referees for their comments and suggestions and A.L. Cruz and A.C.E. Pedretti acknowledges CAPES and CNPq, respectively, for awarding scholarships.

LITERATURE CITED

Bartels H. 1971. Diffusion coefficients and Krogh's diffusion constants. In: Altman PL, Dittmer DS, editors. Respiration and Circulation. Biological Handbooks. Bethesda: FASEB. pp 21–22.

Biswas N, Ojha J, Munshi JSD. 1981. Morphometrics of the respiratory organs of an estuarine goby, *Boleophthalmus boddaerti*. J Ichthyol 27:316–326.

Burri PH, Haeni B, Tschanz AS, Makanya AN. 2003. Morphometry and allometry of the postnatal marsupial lung development: An ultrastructural study. Resp Physiol Neurobiol 138: 309–324.

Carter GS, Beadle LC. 1931. The fauna of the swamps of Paraguayan Chaco in relation to its environment. II. Respiratory adaptations in the fishes. J Linn Soc London (Zool) 37:327–368.

Crawford RH. 1974. Structure of an air-breathing organ and the swim bladder in the Alaskan blackfish, *Dallia pectorallis* Bean. Can J Zool 52:1221–1225.

Cruz AL. 2007. O comportamento respiratório e a cascata de O_2 no cascudo de respiração bimodal *Pterygoplichthys anisitsi* Eigenmann e Kennedy, 1903 (Teleostei, Loricariidae). PhD Thesis. São Carlos: Universidade Federal de São Carlos. 161 p.

Daniels CB, Orgeig S. 2001. The comparative biology of pulmonary surfactant: Past, present and future. Comp Biochem Physiol A 129:9–36.

Daniels CB, Orgeig S, Smits AW. 1995. The evolution of the vertebrate pulmonary surfactant. Physiol Zool 68:539–566.

Daniels CB, Orgeig S, Sullivan LC, Ling N, Bennett MB, Schürch S, Val AL, Brauner CJ. 2004. The origin and evolution of the surfactant system in fish: Insights into the evolution of lungs and swim bladders. Physiol Biochem Zool 77:732–749.

Delariva RL, Agostinho AA. 2001. Relationship between morphology and diets of six neotropical loricariids. J Fish Biol 58:832–847.

Elbal MT, Agullero B. 1986. A histochemical and ultrastructural study of the gut of *Sparus auratus* (Teleostei) J Submicrosc Cytol 18:335–347.

Gee JH. 1976. Buoyancy and aerial respiration: Factors influencing the evolution of reduced swim-bladder volume in some Central American catfishes (Trichomycteridae, Callichthyidae, Loricariidae, Astroblepidae). Can J Zool 54:1030–1037.

Gee JH, Graham JB. 1978. Respiratory and hydrostatic functions of the intestine of the catfishes *Hoplosternum thoracatum* and *Brochis splendens* (Callichthyidae). J Exp Biol 74:1–16.

Graham JB. 1997. Air-Breathing Fishes: Evolution, Diversity, and Adaptation. San Diego: Academic Press. 299 p.

Gundersen HJG, Bendtsen TF, Korbo L. 1988. Some new simple and efficient stereological methods and their use in pathological research and diagnosis. Acta Pathol Microbiol Immunol Scand 96:379–394.

Hakin A, Munshi JSD, Hughes GM. 1978. Morphometrics of the respiratory organs of the Indian green snake-headed fish, *Channa punctata*. J Zool (London) 184:519–543.

Howard CV, Reed MG. 1998. Unbiased Stereology: Three-Dimensional Measurement in Microscopy. Oxford: Bios Scietific Publishers. 246 p.

Hughes GM, Weibel ER. 1976. Morphometry of fish lungs. In: Hughes GM, editor. Respiration of Amphibious Vertebrates. London: Academic Press. pp 213–231.

Hughes GM, Singh BR, Guha G, Dube SC, Munshi JSD. 1974a. Respiratory surface areas of an air-breathing siluroid fish *Heteropneustes fossilis* in relation to body size. J Zool (London) 172:215–232.

Hughes GM, Singh BR, Thakur RN, Munshi JSD. 1974b. Areas of the air-breathing surfaces of *Amphipnous cuchia* (Ham). Proc Indian Nat Sci Acad 40:379–392.

Kemp NE. 1987. The biology of the Australian lungfish, *Neoceratodus forsteri*. In: Bemis WE, Burggren WW, Kemp NE, editors. The Biology and Evolution of Lungfishes. New York: Alan R. Liss. pp 181–198.

Kramer DL. 1978. Ventilation of the respiratory gas bladder in *Hoplerythrinus unitaeniatus* (Pisces, Characoidei, Erythrinidae). Can J Zool 56:931–938.

Liem KF. 1989. Respiratory gas bladder in teleosts: Functional conservatism and morphological diversity. Am Zool 29:333–352.

Maina JN, Maloiy GMO. 1985. The morphometry of the lung of the African lungfish (*Protopterus aethiopicus*): Its structural-functional correlations. Proc R Soc Lond Biol Sci 224:399–420.

Maina JN, West JB. 2005. Thin and strong! The bioengineering dilemma in the structural and functional design of the blood-gas barrier. Physiol Rev 85:811–844.

Mattias AT, Moron SE, Fernandes MN. 1996. Aquatic respiration during hypoxia of the facultative air-breathing *Hoplerythrinus unitaeniatus*. A comparison with the water-breathing *Hoplias malabaricus*. In: Val AL, Almeida-Val VM, Randall DJ, editors. Physiology and Biochemistry of the Fishes of the Amazon. Manaus: INPA. pp 203–209.

McMahon BR, Burggren WW. 1987. Respiratory physiology of intestinal air breathing in the teleost fish *Misgurnus anguillicaudatus*. J Exp Biol 133:371–393.

Moraes MFPG, Höller S, Costa OTF, Glass ML, Fernandes MN, Perry SF. 2005. Morphometric comparison of the respiratory organs of the South American lungfish *Lepidosiren paradoxa* (Dipnoi). Physiol Biochem Zool 78:546–559.

Morrison CM, Wright JR Jr. 1999. A study of the histology of the digestive tract of the Nile tilapia. J Fish Biol 54:597–606.

Munshi JSD. 1985. The structure, function and evolution of the accessory respiratory organs of air-breathing fishes of India. Fortsch Zool 30:353–366.

Munshi JSD, Hughes GM, Gehr P, Weibel ER. 1989. Structure of the air-breathing organs of a swamp mud eel *Monopterus cuchia*. Japan J Ichthyol 35:453–465.

Oliveira C, Taboga SR, Smarra ALS, Bonilla-Rodriguez GO. 2001. Microscopical aspects of acessory air breathing through

a modified stomach in the armoured catfish *Liposarcus anisitsi* (Siluriformes. Loricariidae). Cytobios 105:153–162.

Orgeig S, Daniels CB. 2001. The roles of cholesterol in pulmonary surfactant: Insights from comparative and evolutionary studies. Comp Biochem Physiol A 129:75–89.

Perry SF. 1989. Structure and function of the reptilian respiratory system. In: Wood SC, editor. Comparative Pulmonary Physiology, Current Concepts. New York: Marcel Dekker. pp 193–236.

Perry SF. 1992. Morphometry of vertebrate gills and lungs: A critical review. In: Egginton S, Ross HF, editors. Modelling of Oxygen Transport from Environment to Cell. SEB Seminar Series 51. Cambridge: Cambridge University Press. pp 57–77.

Podkowa D, Goniakowska-Witalinska L. 1998. The structure of the airbladder of the catfish *Pangasius hypophthalmus* Roberts and Vidthayanon 1991, (previously *P. sutchi* Fowler 1937). Folia Biol 46:189–196.

Podkowa D, Goniakowska-Witalinska L. 2002. Adaptations to the air breathing in the posterior intestine of the catfish (*Corydoras aeneus*, Callichthyidae): A histological and ultrastructural study. Folia Biol 50:69–82.

Podkowa D, Goniakowska-Witalinska L. 2003. Morphology of the air-breathing stomach of the catfish *Hypostomus plecostomus*. J Morphol 257:147–163.

Rubio S, Chailley-Heu B, Ducroc R, Bourbon JR. 1996. Antibody against pulmonary surfactant protein A recognizes proteins in intestine and swim bladder of the freshwater fish, carp. Biochem Biophys Res Commun 225:901–906.

Satora L. 1998. Histological and ultrastructural study of the stomach of the air-breathing *Ancistrus multispinnis* (Siluriformes, Teleostei). Can J Zool 76:83–86.

Satora L, Winnicki A. 2000. Stomach as an additional respiratory organ, as exemplified by *Ancistrus multispinnis* (Couvier et Valenciennes, 1937). Siluriformes, Teleostei. Acta Icht Piscat 30:73–79.

Sawaya P. 1946. Sobre a biologia de alguns peixes de respiração aérea (*Lepidosiren paradoxa* Fitzinger e *Arapaima gigas* Cuvier). Bol Fac Fil Cienc Let Univ São Paulo 11:255–286.

Scotto P, Ichinose Y, Patané L, Meyer M, Piiper J. 1987. Alveolar-capillary diffusion of oxygen in dogs exercising in hypoxia. Resp Physiol 68:1–10.

Silva JM, Hernandez-Blazquez FJ, Julio HF Jr. 1997. A new accesory respiratory organ in fishes: Morphology of the respiratory purses of *Loricariichthys platymetopon* (Pisces, Loricariidae). Ann Sci Natur Zool 18:93–103.

Weibel ER. 1999. Understanding the limitation of O_2 supply through comparative physiology. Resp Physiol 118:85–93.

Weibel ER, Knight BW. 1964. A morphometric study on the thickness of the pulmonary air-blood barrier. J Cell Biol 21:367–384.